Accepted Manuscript

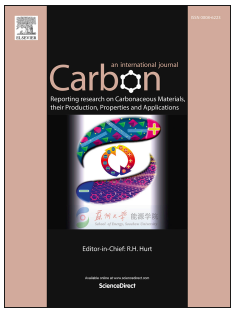

Fluorescence from graphene nanoribbons of well-defined structure

S. Zhao, L. Rondin, G. Delport, C. Voisin, U. Beser, Y. Hu, X. Feng, K. Müllen, A. Narita, S. Campidelli, J.S. Lauret

PII: S0008-6223(17)30409-8

DOI: 10.1016/j.carbon.2017.04.043

Reference: CARBON 11952

To appear in: *Carbon*

Received Date: 10 February 2017

Revised Date: 30 March 2017

Accepted Date: 19 April 2017

Please cite this article as: S. Zhao, L. Rondin, G. Delport, C. Voisin, U. Beser, Y. Hu, X. Feng, K. Müllen, A. Narita, S. Campidelli, J.S. Lauret, Fluorescence from graphene nanoribbons of well-defined structure, *Carbon* (2017), doi: 10.1016/j.carbon.2017.04.043.

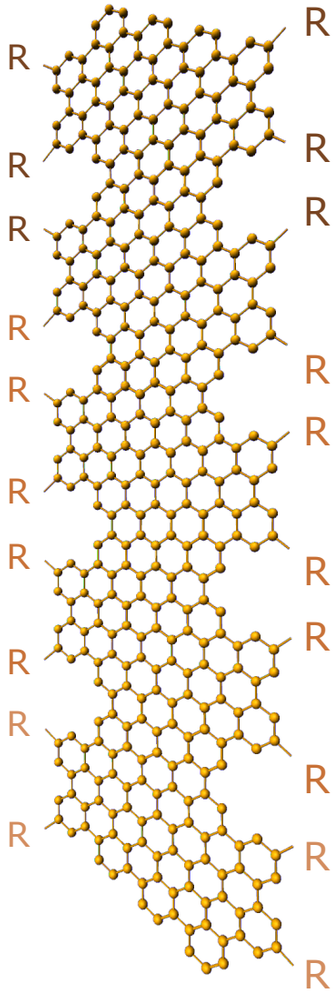

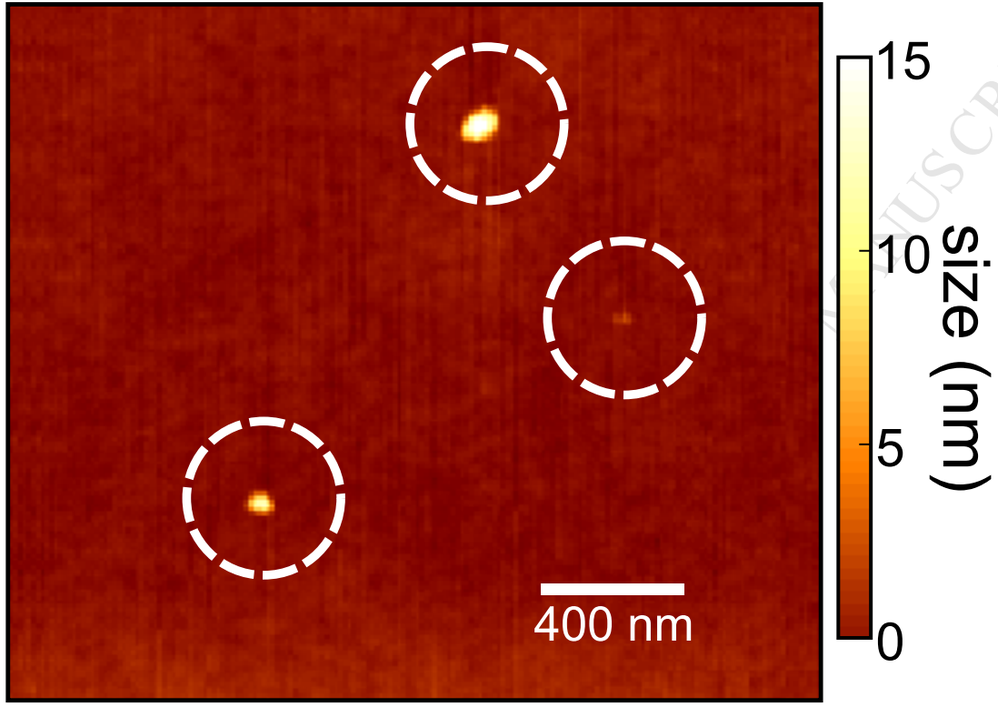

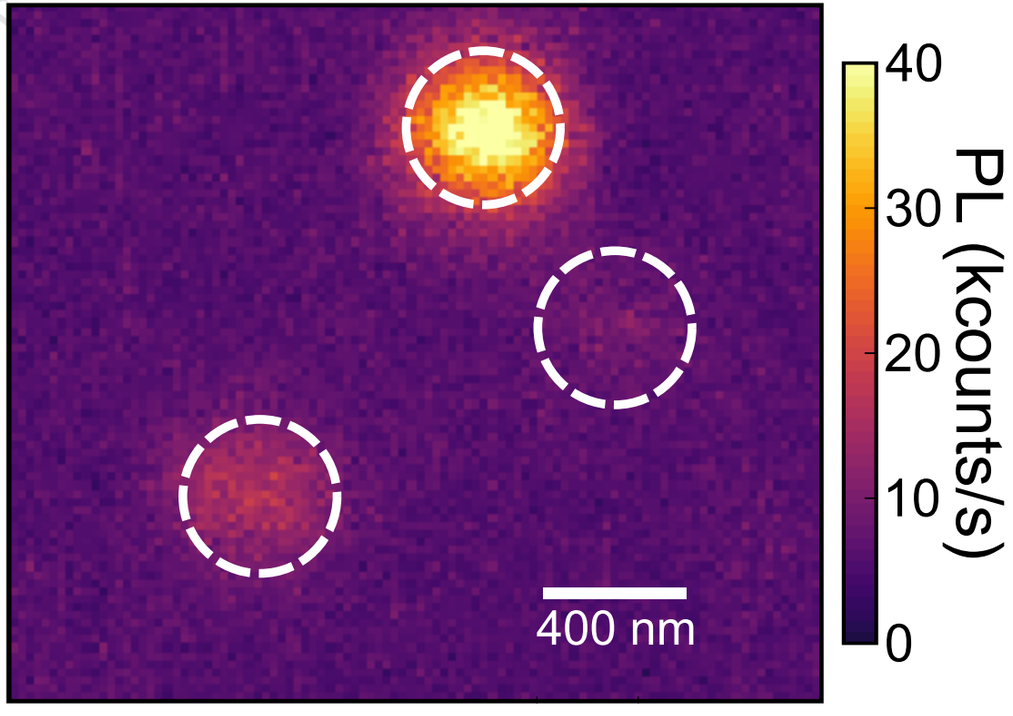

Fluorescence from graphene nanoribbons of well-defined structure.

S. Zhao[a], L. Rondin[a], G. Delport[a], C. Voisin[b], U. Beser[c], Y. Hu[c], X. Feng[d], K. Müllen[c], A. Narita[c], S. Campidelli[e], J.S. Lauret[a,*]

[a]*Laboratoire Aimé Cotton, ENS Cachan, CNRS, Université Paris Sud, bat 505 campus d'Orsay, 91405 Orsay cedex France*
[b]*Laboratoire Pierre Aigrain, École Normale Supérieure, CNRS (UMR8551), Université Pierre et Marie Curie, Université Paris Diderot, 24 rue Lhomond F75005 Paris, France*
[c]*Max Planck Institute for Polymer Research Ackermannweg 10, 55128 Mainz, Germany*
[d]*Technische Universitaet Dresden, Center for Advancing Electronics Dresden and Department of Chemistry and Food Chemistry, Dresden, 01062, Germany*
[e]*LICSEN, NIMBE, CEA, CNRS, Université Paris-Saclay, CEA Saclay 91191 Gif-sur-Yvette Cedex, France*

Abstract

Graphene nanoribbons synthesized by the bottom-up approach with optical energy gaps in the visible are investigated by means of optical spectroscopy. The optical absorption and fluorescence spectra of two graphene nanoribbons with different structures are reported as well as the life-time of the excited states. The possibility of the formation of excimer states in stacks of individual graphene nanoribbons is discussed in order to interpret the broad and highly Stokes-shifted luminescence lines observed on both structures. Finally, combined atomic force microscopy and confocal fluorescence measurements have been performed on small aggregates, showing the ability of graphene nanoribbons to emit light in the solid state. These observations open interesting perspectives for the use of graphene nanoribbons as near-infrared emitters.

1. Introduction

In the last decade, research on graphene has been extensively developed. It is now well established that graphene shows unique physical properties, as represented by the exceptionally high charge-carrier mobility. It demonstrates promises for a wealth of applications such as electrode for energy storage applications, for composites, sensing or electronics[1]. However, graphene is a zero-bandgap semiconductor. Therefore, a lot of studies have been carried out to develop graphene-like semiconductors with large bandgaps. In this context, graphene nanoribbons (GNRs) are promising materials that enable applications in carbon electronics and optoelectronics [2–4]. Indeed, these nano-objects have strong assets such as the tunability of most of their properties by controlling the width and edges structure[3, 5, 6]. For example, the engineering of the edges provides a control on a wide variety of properties: gap energy, electronic band structure, optical selection rules, magnetic order, etc...[3, 7–9] For instance, zigzag edged GNRs are predicted to possess a magnetic localized edge state with negligible bandgaps, whereas the addition of a benzo-fused edge (see figure 1(a)) leads to the disappearance of the edge state and the opening of a ∼2.25 eV bandgap[3].

Harnessing the great potential of these objects is only possible through a precise control of their structure. In the last decade, most of the synthesis methods of GNRs have been based on "top-down" approaches[10, 11]. These processes, which often rely on lithographic or oxidative routes, are not suitable to produce GNRs with small widths (< 10 nm) and lead to uncontrolled edge structures. In the perspective of reaching a fine control of the GNR geometry, the bottom-up chemical synthesis of long GNRs with defined structures represents a major breakthrough[12–16]. It opens the possibility to obtain a variety of desired structures by correctly designing specific precursors and the assembly route. Recently, significant progresses have been made in the GNRs synthesis. For instance, armchair edge GNRs with various widths, "cove"-type edge GNRs, and even zigzag edge GNRs showing the theoretically predicted localized states have been achieved[13, 15]. The electronic properties of the GNRs have been intensively studied e.g., by scanning tunneling spectroscopy, angle-resolved photoelectron spectroscopy, high-resolution electron energy loss spectroscopy, and fabrication of field-effect transistor devices[17–19]. In contrast, there is an obvious lack of knowledge about their optical properties. Optical absorption spectroscopy has been reported, showing the dependence of the gap on the width of the GNR[12, 14, 20–22]. The comparison between reflectivity measurements on GNRs grown on gold and *ab-initio* calculations recently highlighted the excitonic nature of the optical transitions, with exciton binding energy as high as 1.5-1.8 eV[23]. Likewise, pump/probe ultrafast transient absorption experiments demonstrated exciton-exciton annihilation and biexciton stimulated emission, with a bi-exciton binding

*Corresponding author
Email address: jean-sebastien.lauret@lac.u-psud.fr (J.S. Lauret)

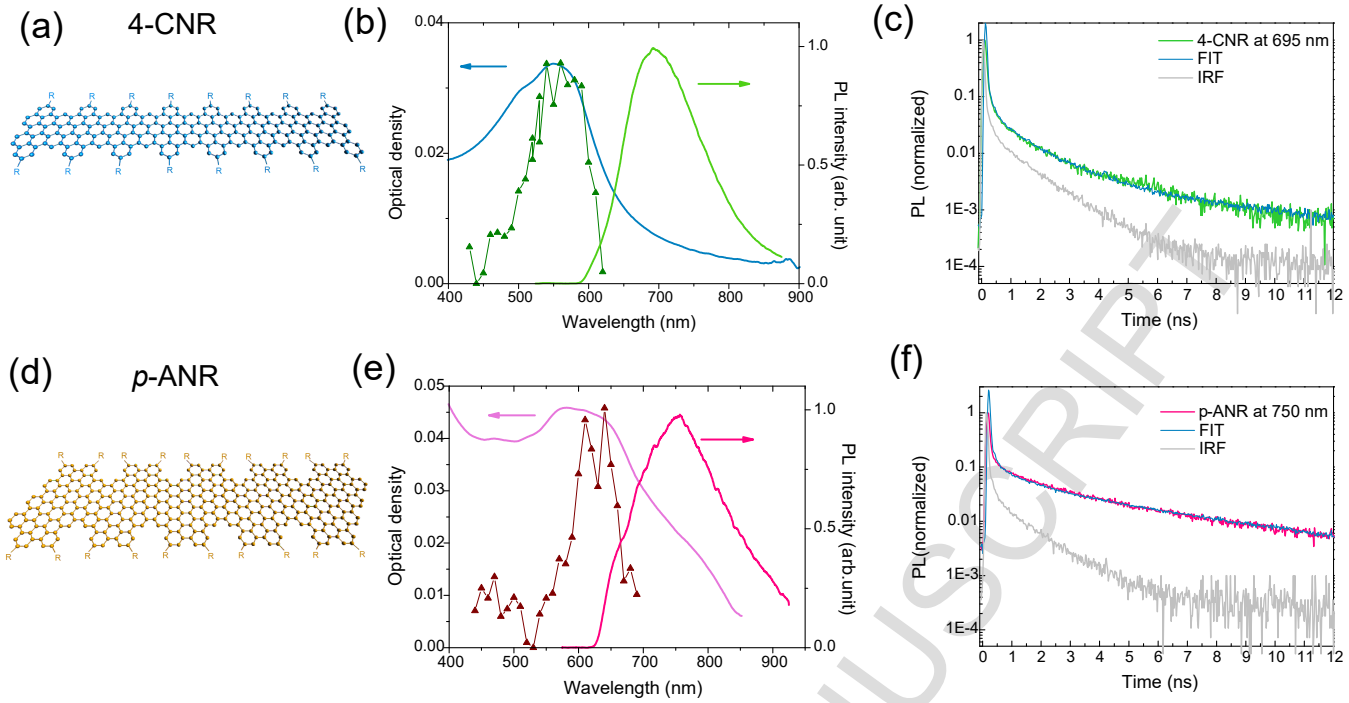

Figure 1: Chemical structures of the 4-CNR (a) and *p*-ANR (d). Optical absorption spectra, photoluminescence and photoluminescence excitation spectra (triangles) of 4-CNR (b) and *p*-ANR (e) in SDS. Time-resolved photoluminescence decay of 4-CNR (c) and *p*-ANR (f). PLE spectra are recorded at the maximum of each PL line.

energy of ∼250 meV[24]. Nevertheless, the photoluminescence (PL) properties of GNRs have remained largely underexplored[22, 25].

In this paper we report on a detailed study of the PL properties of two bottom-up-synthesized GNRs with defined structures, namely 4-CNR and *p*-ANR[14, 22], following the name code used in Ref [3]. Both GNRs show broad PL lines and a large Stokes shift. The PL line of *p*-ANR is red-shifted in comparison with that of 4-CNR due to a larger width of the ribbon leading to a lower degree of confinement. Multi-exponential decays are measured by means of time-resolved PL (TR-PL) experiments with life-time ranging from few ps to few ns. Finally, very small GNRs aggregates have been investigated simultaneously by confocal microscopy and atomic force microscopy, revealing their optical properties in the solid state.

2. Experimental

The suspensions of GNRs are made by tip-sonication (∼1h30) in water with 2%wt of sodium dodecyl sulfate. Same experiments with sodium cholate lead to comparable results (see optical absorption spectrum in ESI). Moreover, different duration and type of sonication (bath, tip) has been used without any reliable difference on the optical spectra. For the purpose of single object measurements, the suspension is drop-casted on the top of a coverslip and then rinsed several times to get rid of the excess of surfactant.

Optical absorption spectroscopy is performed on a PerkinElmer Lambda 950 spectrophotometer. In PL/PLE and TR-PL spectroscopy experiments in suspension, the sample is excited with the white light of a supercontinuum laser (Fianium) filtered by a monochromator (Ropers Scientific SP2150i). The PL spectra are analyzed in a SP2500i (Roper Scientific) spectrometer equipped with a CCD camera (PIXIS 100 model: 7515-0002). Finally, time correlated single photon counting was used to perform the luminescence life-time measurements (TR-PL).

AFM images were recorded in tapping mode using an Asylum Research MFP-3D AFM. The AFM system is combined with an inverted confocal microscope allowing simultaneous AFM and PL imaging of the sample. The luminescence is excited by a Cobolt Mambo 100 594 nm laser and collected through the same oil immersion objective (x60, NA = 1.42). The luminescence is split from excitation laser using a dichroic mirror (Chroma ZT594rdc) and filtered using a longpass filter (Semrock BLP01-635R-25). The luminescence is then redirected rather on an avalanche photodiode in the single photon counting regime (PerkinElmer SPCM-AQR-13) or to a spectrograph (Ropers Scientific SP2150i)

3. Results and discussion

4-CNR and *p*-ANR were prepared adapting reported procedures, through the solution-mediated intramolecular oxidative cyclodehydrogenation, or "graphitization", of

tailor-made polyphenylene precursors [14, 22, 26]. Raman and FTIR spectra of both GNR samples were in agreement with our previous reports, which supported their GNR structures (see figure S7 and S8 in ESI)[14, 22]. The first structure studied in this paper, 4-CNR, is described on figure 1(a). 4-CNR has a structure based on $N = 4$ zigzag edge GNRs with additional benzo-fused rings, where N stands for the number of carbon atoms across the nanoribbon[3]. It forms a "cove"-type edge configuration that leads to a semiconducting nanostructure with a visible gap[3]. Alkyl groups (-$C_{12}H_{25}$) are added on the edges in order to improve the dispersibility of GNRs. Figure 1(b) displays the optical absorption spectrum of 4-CNR in suspension in water with 2%wt of sodium dodecyl sulfate (SDS) (blue curve). An absorption band centred at 560 nm (∼2.21 eV) is observed, in good agreement with previous reports[14, 24]. This exciton line is supposed to be mainly formed by the E_{21} transition between the top of the second valence band and the bottom of the first conduction band of 4-CNR[24]. Moreover, figure 1(b) shows the photoluminescence (PL) spectrum of the 4-CNR suspension (green curve). The PL line is broad, structureless, and centred at 695 nm (∼1.78 eV). The difference between the maxima of the absorption and PL bands represents an apparent Stokes shift of ∼135 nm (∼470 meV). The full width at half maximum (FWHM) is ∼105 nm (∼330 meV). The values of the Stokes shift and of the FWHM will be discussed later in the paper. The photoluminescence excitation (PLE) spectrum detected at the maximum of the PL line is plotted on Figure 1(b)(green triangles). The PLE fits quite well with the absorption band, confirming that the observed Stokes shifted luminescence arises from the GNRs. Finally, time-resolved PL (TR-PL) has been performed. Results are displayed on figure 1(c)(green curve) together with the impulse response function (IRF). The PL decay is slightly longer than the IRF of the setup (∼70 ps). The signal has been fitted with a bi-exponential decay with a fast time of the order of few ps and a long time of ∼5 ns (see blue curve in figure 1 (c)).

We have also investigated p-ANR, which is based on $N = 9$ armchair GNR with partially extended edges having the width of $N = 15$ armchair GNR at the widest (see figure 1(d))[22]. This GNR geometry shows a near-infrared gap. Figure 1(e) displays the optical absorption spectrum of the p-ANR suspension. The absorption band is red-shifted in comparison with the one of 4-CNR, with a maximum at ∼610 nm, in good agreement with the larger delocalization of the π electrons of p-ANRs. As for 4-CNR, the PL of p-ANR is broad (FWHM 170 nm (∼360 meV)) with a large Stokes Shift of 145 nm (∼400 meV). Likewise, the PLE spectrum shows that the maximum of PL efficiency is obtained for an excitation in resonance with the maximum of the absorption band. Finally, the TR-PL shows also a multiexponential decay with a more pronounced signal at long times than on 4-CNR. In the case of p-ANR, the bi-exponential decay is also fitted with a short time of few ps and a long time of ∼5 ns.

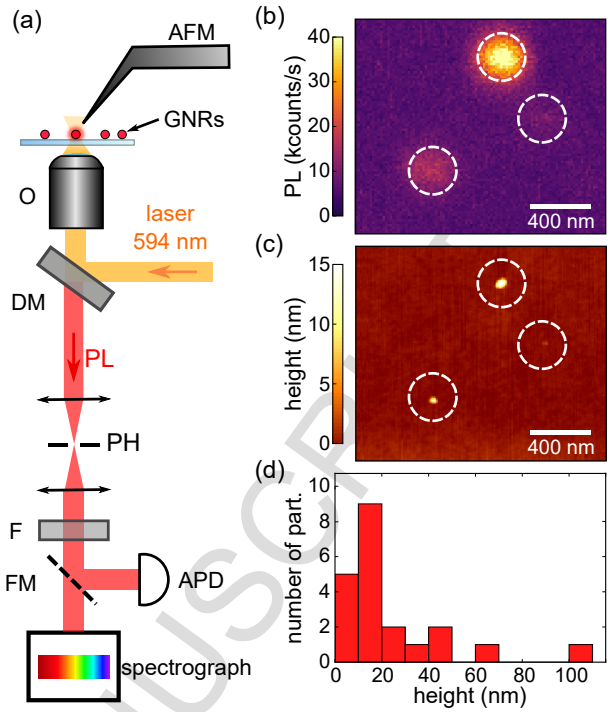

Figure 2: AFM and PL characterization of small p-ANR aggregates. (a) Experimental setup combining an AFM and an homebuilt confocal microscope. The detected luminescence through the oil immersion objective O can be sent rather to a silicon avalanche photodiode (APD) or to a spectrograph. DM stands for dichroic mirror, F for a longpass 635 nm filter. (b) and (c) - PL image (b) and corresponding AFM image (c) of GNRs deposited on a glass coverslip. White dots highlight three luminescent GNRs small aggregates, with heights of 2.5, 13 and 17 nm. (d) histogram of the height of the luminescent particles on this particular sample.

The nature of the emission of both GNR structures will be now discussed. First, the PL of 4-CNR and p-ANR share similar behaviors: broad emission, large Stokes shift and multi-exponential decays. These observations differ significantly from what is observed on other 1D carbon nanostructures. For instance, single wall carbon nanotubes (SWNT) emission shows almost no Stokes shift and the linewidth of a single chirality is of the order of 25 nm (∼25 meV)[27–29]. Likewise, conjugated polymers show intrinsic fluorescence with a small Stokes shift and a mono-exponential decay. If the observed luminescence of GNRs were intrinsic, one would have to invoke complicated vibronic structures and complex internal relaxation path- ways to lead to such broad and Stokes-shifted emission and multiexponential decay.

The most natural explanation would be then to attribute the fluorescence to defect states in the GNRs structure. These defect states can arise from the presence of defects at the edges, from open-bonds or from the lateral alkyl chains (-$C_{12}H_{25}$, see figure 1(a) and (d)). The presence of defects located on the edges of the GNRs can be ruled out due to the fabrication process of our GNRs. The perfectly controlled structure enforced by organic chemistry prevents the appearance such major defects that are,

for instance, responsible for the PL of graphene quantum dots synthesized by a top-down route[30]. Concerning sp^3 carbon defects due to open bonds, they are likely to lead to a fluorescence at higher energy. Therefore, they can not account for the red-shifted emission reported here on both structures. The expected effects of lateral alkyl chains on the electronic structure and optical properties of GNRs are more complex and of keen interest. Indeed, our recent theoretical and experimental studies on the Raman spectra of such GNRs, including 4-CNRs, revealed significant effects of the alkyl chains on their vibrational properties[31]. For instance, the alkyl chains modifies the radial-like breathing mode frequency. It is therefore interesting to question on the influence of these chains on the electronic structure. The replacement of one hydrogen atom of the edge by the carbon chain could, for instance, create new states in the energy gap of GNRs. However, a recent theoretical work by C.E.P. Villegas et al. shows that side chains should have no influence on the optical properties of 4-CNRs [32]. So, the presence of these alkyl chains can not explain our observations.

On the other hand, despite the presence of the alkyl chains, the molecular solubilization of GNRs is challenging[22]. We decided to use water/SDS suspension since this it has been successful for the individualization of SWNT and it permits to use tip sonication[27]. Nevertheless, it is likely that aggregates are present in the GNR suspensions used in these experiments. Indeed, π-conjugated object are known to self-aggregate through $\pi-\pi$ interaction, even at moderate concentrations[33]. Moreover, in some cases the aggregation leads to a vibronic coupling between monomers (single isolated molecule) that results in strong modifications of their spectroscopic features. For instance, excimer emission has been reported on aggregates of small conjugated molecules such as pyrene, in conjugated polymers or in hexabenzocoronene[33–36]. An excimer corresponds to the coupling between a monomer M_g in its ground state and a monomer M_{ex} in its excited states that form an excited dimer D_{ex}. The system returns back to equilibrium when D_{ex} dissociate in the ground state leading to a broad, structureless PL at much lower energy than the monomer absorption. Excimers occur when monomers stack together in sandwich-type configuration[37]. The most known system showing excimer emission is the pyrene molecule that emits excimer fluorescence near ∼485 nm when the concentration is increased[38]. The excimer emission is broad, structureless and red-shifted of ∼80 nm (∼490 meV) in comparison with that of the monomer. Similarly, excimer emission has been observed on stacks of π-conjugated polymers leading to a multi-exponential decay, with apparent Stokes-shift of ∼100 nm (∼500 meV) [37]. Likewise, hexabenzocoronene derivatives, which are studied as model systems for graphene, tend to form aggregates in suspension though face to face $\pi-\pi$ interaction. Here again, this coupling results in a broad emission that is red-shifted in comparison with the one of the monomers, and that has been therefore attributed to an excimer-like emission[35, 36]. Given their structure, GNRs are likely to stack in the sandwich-type configuration. Since the PL of both GNR structures reported here share very similar characteristics with the one reported for those π-conjugated objects, it sounds reasonable to attribute it, at least partially, to the formation of excimers.

Nevertheless, despite their global similarities, some features of *p*-ANR optical response differ from that of 4-CNR. First, an additional absorption band is observed on the red side of the main transition around 790 nm. This shoulder could be related to an intrinsic transition. Indeed, it has been predicted theoretically that *p*-ANR should exhibit a much complex peak structure than 4-CNR[3]. In that case, the PL line observed on *p*-ANR could be closed to that of single isolated GNR. This could also be in good agreement with the longer average lifetime of *p*-ANR in comparison with that of 4-CNR. On the contrary, the shoulder in the absorption spectrum of *p*-ANR could also be related to a much more pronounced aggregation than for 4-CNR. Indeed, it has been demonstrated, for instance on hexabenzocoronene, that a high degree of aggregation could lead to such feature in absorption spectroscopy[36].

Since measurements on ensemble of objects are subject to averaging effects, experiments at the single particle level have been performed in order to investigate close-to intrinsic properties of the GNRs. The suspension of *p*-ANRs has been deposited by dropcasting on the surface of a coverslip. The sample has been then analysed on a confocal microscopy setup that is coupled to an atomic force microscope (AFM) (see figure 2(a)). First, a statistics of the height measured by AFM is displayed on figure 2(d). It shows that the height of most of the objects deposited from the suspension is in the range of 10 to 20 nm. This observation supports the presence of small GNR aggregates in the suspension. Figure 2(c) shows a typical $1\mu m \times 1\mu m$ AFM image. Three small aggregates (white dashed circles) are present in this area with heights ranging from ∼17 nm to ∼2.5 nm (see figure S2 of the ESI). The very same location of the sample has been scanned by fluorescence confocal microscopy. Figure 2(b) displays this fluorescence map which demonstrates that the three small GNR aggregates emit light. This observation demonstrates the ability of GNRs to emit light in the solid state. Other co-localization scans (AFM and fluorescence microscopy) are displayed in ESI. Moreover, the PL signal of the GNRs aggregates are quite stable over time (see figure S4 of ESI).

Finally, figure 3 represents typical spectra recorded on small aggregates by microphotoluminescence spectroscopy. Each spectrum has been acquired on different spots on the sample. First, the stars in figure 3 point some lines that corresponds to Raman mode characteristic of sp^2 carbon nanostructures at 2619 ± 20 cm^{-1} (2D), 2934 ± 20 cm^{-1} (D+D') and 3195 ± 20 cm^{-1} (2G) from the laser line[12]. This observation strongly supports that the emission spots observed by fluorescence spectroscopy do correspond to the emission of GNRs. The spectra of those three aggre-

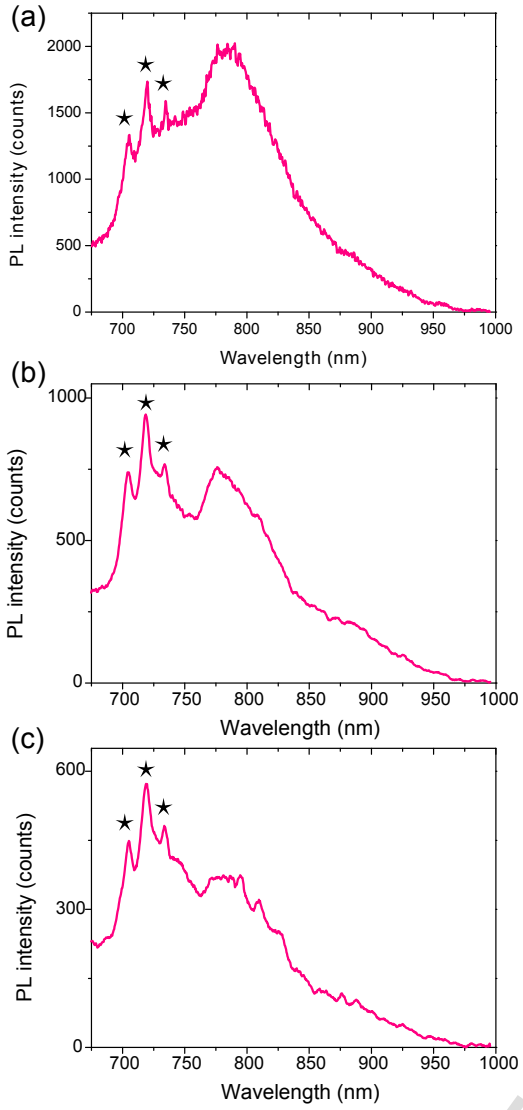

Figure 3: Typical spectra observed on three p-ANR aggregates with an excitation at 594 nm (a) 45 nm (b) 25 nm (c) 15 nm. The stars refer to Raman lines (see text for details).

gates show similar Stokes shift to the one observed in suspensions (see ESI for the direct comparison). Therefore, this red-shifted fluorescence emitted by aggregates is consistent with an excimer emission. Furthermore, the shape of the PL line is varying from one spot to another. Sometimes a contribution centered at ∼795 nm dominates the spectrum (figure 3(a)). For another aggregate, the main line is centered at ∼725 nm (figure 3(c)), closer to the absorption edge. Finally, intermediate cases are also observed (figure 3(b)). This variety observed in the PL spectra of individual aggregates shows that PL line recorded in suspension is inhomogeneously broadened. Finally, on a statistic of about twenty aggregates, no correlation between the height of the particle and the shape of the spectrum, nor its intensity, have been put in evidence.

4. Conclusion

In summary, we reported on the optical properties of 4-CNR and p-ANRs synthesized by bottum-up chemistry. The broad and highly Stokes shifted emission of both structures and its multiexponential decay may originate from excimer states in stacks of individual GNRs. Moreover, the emission of very small aggregates at the solid state has been observed by means of AFM and confocal microscopy. Raman lines are superimposed on the fluorescence signal confirming the sp^2 nature of the emitter. In this work, we show that this kind of suspensions are mainly composed of small aggregates that blur the intrinsic properties of GNR. It highlights the need of further work to obtain well individualized GNRs that is a prerequisite to be able to take advantage of the great possibilities of those nanoobjects. To reach this goal, several strategies are currently developed. Among them, the study of single GNRs grown directly on gold surface and then transferred on an appropriate substrate sounds very promising and is currently pursued in our laboratories.

5. Acknowledgment

The authors are grateful to Thomas Hingant for his help on the data processing, and to V. Jacques for helpful discussions. This work is supported by the GDR-I GNT, DFG Priority Program SPP 1459, the European Commission through the FET-Proactive Project "MoQuaS" (contract number 610449) and Graphene Flagship, and the Chinese Government Scholarship (CSC) under grant 201508070071. J.S.Lauret is a member of "Institut Universitaire de France".

[1] K. Novoselov, V. I. Falko, L. Colombo, P. Gellert, M. Schwab, K. Kim, A roadmap for graphene, Nature 490 (2012) 192–200. doi:10.1038/nature11458.
[2] K. Müllen, Evolution of graphene molecules: Structural and functional complexity as driving forces behind nanoscience, ACS Nano 8 (Xx) (2014) 6531–6541. doi:10.1021/nn503283d.
[3] S. Osella, A. Narita, M. G. Schwab, Y. Hernandez, X. Feng, Graphene Nanoribbons as Low Band Gap Donor Materials for Organic Photovoltaics: Quantum Chemical Aided Design, ACS Nano 6 (6) (2012) 5539–5548.
[4] F. Bonaccorso, Z. Sun, T. Hasan, A. C. Ferrari, Graphene photonics and optoelectronics, Nature Photonics 4 (9) (2010) 611–622.
[5] J. Wang, R. Zhao, M. Yang, Z. Liu, Z. Liu, Inverse relationship between carrier mobility and bandgap in graphene, The Journal of Chemical Physics 138 (8) (2013) 084701. doi:10.1063/1.4792142.
[6] K. Nakada, M. Fujita, G. Dresselhaus, M. S. Dresselhaus, Edge state in graphene ribbons: Nanometer size effect and edge shape dependence, Phys. Rev. B 54 (1996) 17954–17961. doi:10.1103/PhysRevB.54.17954.
[7] X. Zhu, H. Su, Scaling of Excitons in Graphene Nanoribbons with Armchair Shaped Edges, J. Phys. Chem. A 115 (2011) 11998–12003.
[8] H. Zheng, Z. F. Wang, T. Luo, Q. W. Shi, J. Chen, Analytical study of electronic structure in armchair graphene nanoribbons, Phys. Rev. B 75 (2007) 165414. doi:10.1103/PhysRevB.75.165414.

[9] G. Z. Magda, X. Jin, L. Hagymasi, P. Vancso, Z. Osvath, P. Nemes-Incze, C. Hwang, L. P. Biro, L. Tapaszto, Room-temperature magnetic order on zigzag edges of narrow graphene nanoribbons, Nature 514 (2014) 608–611.

[10] X. Li, X. Wang, L. Zhang, S. Lee, H. Dai, Chemically derived, ultrasmooth graphene nanoribbon semiconductors, Science 319 (5867) (2008) 1229–1232.

[11] M. Zeng, Y. Xiao, J. Liu, W. Lu, L. Fu, Controllable fabrication of nanostructured graphene towards electronics, Advanced Electronic Materials 2 (4) (2016) 1500456, 1500456. doi:10.1002/aelm.201500456.

[12] M. G. Schwab, A. Narita, Y. Hernandez, T. Balandina, K. S. Mali, S. De Feyter, X. Feng, K. Müllen, Structurally Defined Graphene Nanoribbons with High Lateral Extension, Journal of the American Chemical Society 134 (44) (2012) 18169–18172.

[13] P. Ruffieux, S. Wang, B. Yang, C. Sánchez-Sánchez, J. Liu, T. Dienel, L. Talirz, P. Shinde, C. A. Pignedoli, D. Passerone, T. Dumslaff, X. Feng, K. Müllen, R. Fasel, On-surface synthesis of graphene nanoribbons with zigzag edge topology, Nature 531 (5867) (2016) 489–492. doi:10.1038/nature17151.

[14] A. Narita, X. Feng, Y. Hernandez, S. A. Jensen, M. Bonn, H. Yang, I. A. Verzhbitskiy, C. Casiraghi, M. R. Hansen, A. H. R. Koch, G. Fytas, O. Ivasenko, B. Li, K. S. Mali, T. Balandina, S. Mahesh, S. De Feyter, K. Müllen, Synthesis of structurally well-defined and liquid-phase-processable graphene nanoribbons., Nature chemistry 6 (2014) 126–32.

[15] A. Narita, X.-Y. Wang, X. Feng, K. Müllen, New advances in nanographene chemistry, Chem. Soc. Rev. 44 (2015) 6616–6643.

[16] L. Talirz, P. Ruffieux, R. Fasel, On-surface synthesis of atomically precise graphene nanoribbons, Advanced Materials 28 (29) (2016) 6222–6231. doi:10.1002/adma.201505738.

[17] P. B. Bennett, Z. Pedramrazi, A. Madani, Y.-C. Chen, D. G. de Oteyza, C. Chen, F. R. Fischer, M. F. Crommie, J. Bokor, Bottom-up graphene nanoribbon field-effect transistors, Applied Physics Letters 103 (25) (2013) 253114. doi:10.1063/1.4855116.

[18] C. Bronner, S. Stremlau, M. Gille, F. Brauße, A. Haase, S. Hecht, P. Tegeder, Aligning the band gap of graphene nanoribbons by monomer doping, Angewandte Chemie International Edition 52 (16) (2013) 4422–4425. doi:10.1002/anie.201209735.

[19] H. Sakaguchi, S. Song, T. Kojima, T. Nakae, Homochiral polymerization-driven selective growth of graphene nanoribbons, Nature Chemistry 9 (2017) 57–63. doi:10.1038/nchem.2614.

[20] T. H. Vo, M. Shekhirev, D. A. Kunkel, M. D. Morton, E. Berglund, L. Kong, P. M. Wilson, P. A. Dowben, A. Enders, A. Sinitskii, Large-scale solution synthesis of narrow graphene nanoribbons, Nature Communcations 5 (2014) 3189. doi:10.1038/ncomms4189.

[21] G. Li, K.-Y. Yoon, X. Zhong, X. Zhu, G. Dong, Efficient bottom-up preparation of graphene nanoribbons by mild suzukimiyaura polymerization of simple triaryl monomers, Chemistry - A European Journal 22 (27) (2016) 9116–9120. doi:10.1002/chem.201602007.

[22] Y. Huang, Y. Mai, U. Beser, J. Teyssandier, G. Velpula, H. V. Gorp, L. A. Straasø, M. R. Hansen, D. Rizzo, C. Casiraghi, R. Yang, G. Zhang, D. Wu, F. Zhang, D. Yan, S. D. Feyter, K. Müllen, X. Feng, Poly(elthylene oxide) Functionalized Graphene Nanoribbons with Excellent Solution Processability, Journal of the American Chemical Society 138 (2016) 10136–10139. doi:10.1021/jacs.6b07061.

[23] R. Denk, M. Hohage, P. Zeppenfeld, J. Cai, C. a. Pignedoli, H. Söde, R. Fasel, X. Feng, K. Müllen, S. Wang, D. Prezzi, A. Ferretti, A. Ruini, E. Molinari, P. Ruffieux, Exciton-dominated optical response of ultra-narrow graphene nanoribbons., Nature communications 5 (2014) 4253.

[24] G. Soavi, S. D. Conte, C. Manzoni, D. Viola, A. Narita, Y. Hu, G. Cerullo, X. Feng, U. Hohenester, E. Molinari, D. Prezzi, K. Müllen, G. Cerullo, Excitonexciton annihilation and biexciton stimulated emission in graphene nanoribbons, Nature Communications 7 (2016) 11010. doi:10.1038/ncomms11010.

[25] T. H. Vo, U. G. E. Perera, M. Shekhirev, M. Mehdi Pour, D. A. Kunkel, H. Lu, A. Gruverman, E. Sutter, M. Cotlet, D. Nykypanchuk, P. Zahl, A. Enders, A. Sinitskii, P. Sutter, Nitrogen-doping induced self-assembly of graphene nanoribbon-based two-dimensional and three-dimensional metamaterials, Nano Letters 15 (9) (2015) 5770–5777. doi:10.1021/acs.nanolett.5b01723.

[26] Details of the synthesis of *p*-ANR derivative with dodecyl chains will be published elsewhere.

[27] M. J. O'Connell, S. M. Bachilo, C. B. Huffman, V. C. Moore, M. S. Strano, E. H. Haroz, K. L. Rialon, P. J. Boul, W. H. Noon, C. Kittrell, J. Ma, R. H. Hauge, R. B. Weisman, R. E. Smalley, Band gap fluorescence from individual single-walled carbon nanotubes, Science 297 (5581) (2002) 593–596. doi:10.1126/science.1072631.

[28] J. S. Lauret, C. Voisin, G. Cassabois, P. Roussignol, C. Delalande, A. Filoramo, L. Capes, E. Valentin, O. Jost, Bandgap photoluminescence of semiconducting single-wall carbon nanotubes, Physica E: Low-dimensional Systems and Nanostructures 21 (0) (2004) 1057–1060.

[29] S. Berger, C. Voisin, G. Cassabois, C. Delalande, P. Roussignol, X. Marie, Temperature dependence of exciton recombination in semiconducting single-wall carbon nanotubes, Nano Letters 7 (2) (2007) 398–402, pMID: 17256994. doi:10.1021/nl062609p.

[30] Q. Xu, Q. Zhou, Z. Hua, C. Zhang, X. Wang, D. Pan, M. Xiao, Single-Particle Spectroscopic Measurements of Fluorescent Graphene Quantum Dots Single-Particle Spectroscopic Measurements of Fluorescent Graphene Quantum Dots, ACS Nano 7 (2013) 10654–10661.

[31] I. Verzhbitskiy, M. D. Corato, A. Ruini, E. Molinari, A. Narita, Y. Hu, M. G. Schwab, M. Bruna, D. Yoon, S. Milana, X. Feng, K. Müllen, A. C. Ferrari, C. Casiraghi, D. Prezzi, Raman fingerprints of atomically precise graphene nanoribbons, Nano Letters 16 (2016) 3442–3447. doi:10.1021/acs.nanolett.5b04183.

[32] C. E. P. Villegas, P. B. Mendonça, a. R. Rocha, Optical spectrum of bottom-up graphene nanoribbons: towards efficient atom-thick excitonic solar cells, Scientific Reports 4 (2014) 6579. doi:10.1038/srep06579.

[33] M. Kastler, W. Pisula, D. Wasserfallen, T. Pakula, K. Müllen, Influence of alkyl substituents on the solution- and surface-organization of hexa-peri-hexabenzocoronenes, Journal of the American Chemical Society 127 (12) (2005) 4286–4296. doi:10.1021/ja0430696.

[34] A. J. Fleming, J. N. Coleman, A. Fechtenkotter, K. Müllen, W. J. Blau, Intermolecular vibronic coupling in self-assembling molecular nanowires of hexabenzocoronene derivatives, Organic Photonic Materials and Devices V 4991 (2003) 460–466. doi:10.1117/12.475427.

[35] J. M. Englert, F. Hauke, X. Feng, K. Müllen, A. Hirsch, Exfoliation of hexa-peri-hexabenzocoronene in water., Chemical communications (Cambridge, England) 46 (48) (2010) 9194–9196. doi:10.1039/c0cc03849k.

[36] J. M. Hughes, Y. Hernandez, D. Aherne, L. Doessel, K. Mu, B. Moreton, T. W. White, C. Partridge, G. Costantini, A. Shmeliov, M. Shannon, V. Nicolosi, J. N. Coleman, High Quality Dispersions of Hexabenzocoronene in Organic Solvents, Journal of the American Chemical Society 134 (2012) 12168.

[37] S. A. Jenekhe, J. A. Osaheni, Excimers and exciplexes of conjugated polymers, Science 265 (5173) (1994) 765–768.

[38] J. B. Birks, Excimers, Rep. Prog. Phys. 38 (8) (1975) 903.